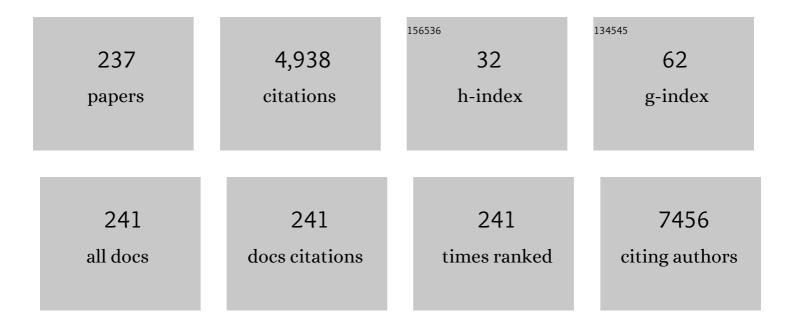
List of Publications by Year in descending order

Source: https://exaly.com/author-pdf/3833144/publications.pdf Version: 2024-02-01



**Δει-κιιενι \λ/ει** 

#	Article	IF	CITATIONS
1	Continuous polymerase chain reaction microfluidics integrated with a gold-capped nanoslit sensing chip for Epstein-Barr virus detection. Biosensors and Bioelectronics, 2022, 195, 113672.	5.3	28
2	Combining portable solar-powered centrifuge to nanoplasmonic sensing chip with smartphone reader for rheumatoid arthritis detection. Chemical Engineering Journal, 2022, 434, 133864.	6.6	11
3	Spectral image contrast-based flow digital nanoplasmon-metry for ultrasensitive antibody detection. Journal of Nanobiotechnology, 2022, 20, 6.	4.2	4
4	A nanofluidic preconcentrator integrated with an aluminum-based nanoplasmonic sensor for Epstein-Barr virus detection. Sensors and Actuators B: Chemical, 2022, 355, 131327.	4.0	11
5	Sensitive Oligonucleotide Detection Using Resonant Coupling between Fano Resonance and Image Dipoles of Cold Nanoparticles. ACS Applied Materials & Interfaces, 2022, 14, 14012-14024.	4.0	13
6	Combination of Capped Gold Nanoslit Array and Electrochemistry for Sensitive Aqueous Mercuric Ions Detection. Nanomaterials, 2022, 12, 88.	1.9	3
7	Sensitive Handheld Refractometer by Using Combination of a Tapered Fiber Tip and a Multimode Fiber. Journal of Lightwave Technology, 2021, 39, 4179-4185.	2.7	2
8	Self-referencing biosensors using Fano resonance in periodic aluminium nanostructures. Nanoscale, 2021, 13, 17775-17783.	2.8	2
9	Screening anti-metastasis drugs by cell adhesion-induced color change in a biochip. Lab on A Chip, 2021, 21, 2955-2970.	3.1	5
10	Dispersion-enhancing surface treatment of AuNPs for a reduced probe loading and detection limit using t-SPR detection. Analyst, The, 2021, 146, 5584-5591.	1.7	3
11	Large shift of resonance wavelengths of silver nanoslit arrays using electrowetting-on-dielectric cells. Optics Letters, 2021, 46, 705.	1.7	7
12	Real-Time Monitoring of Frost/Defrost Processes Using a Tapered Optical Fiber. IEEE Sensors Journal, 2021, 21, 6188-6194.	2.4	4
13	Nanoplasmonic Structure of a Polycarbonate Substrate Integrated with Parallel Microchannels for Label-Free Multiplex Detection. Polymers, 2021, 13, 3294.	2.0	5
14	Enhancing Raman signals from bacteria using dielectrophoretic force between conductive lensed fiber and black silicon. Biosensors and Bioelectronics, 2021, 191, 113463.	5.3	3
15	Polyglutamine-Specific Gold Nanoparticle Complex Alleviates Mutant Huntingtin-Induced Toxicity. ACS Applied Materials & Interfaces, 2021, 13, 60894-60906.	4.0	3
16	<i>LMP1</i> gene detection using a capped gold nanowire array surface plasmon resonance sensor in a microfluidic chip. Analyst, The, 2020, 145, 52-60.	1.7	24
17	Multichannel nanoplasmonic platform for imidacloprid and fipronil residues rapid screen detection. Biosensors and Bioelectronics, 2020, 170, 112677.	5.3	22
18	Promising urinary miRNA biomarkers t-SPR profiling for urothelial cell carcinoma. Sensors and Actuators B: Chemical, 2020, 322, 128605.	4.0	9

#	Article	IF	CITATIONS
19	Spectrally selective photodetection in the near-infrared with a gold grating-based hot electron structure. Applied Physics Letters, 2020, 116, .	1.5	20
20	Hot electron photodetection with spectral selectivity in the C-band using a silicon channel-separated gold grating structure. Nano Express, 2020, 1, 010015.	1.2	1
21	High-Throughput and Dynamic Study of Drug and Cell Interactions Using Contrast Images in Aluminum-Based Nanoslit Arrays. Analytical Chemistry, 2020, 92, 9674-9681.	3.2	11
22	Impedimetric aptasensing using a symmetric Randles circuit model. Electrochimica Acta, 2020, 337, 135750.	2.6	8
23	A Concave Blazed-Grating-Based Smartphone Spectrometer for Multichannel Sensing. IEEE Sensors Journal, 2019, 19, 11134-11141.	2.4	24
24	Spectral contrast imaging method for mapping transmission surface plasmon images in metallic nanostructures. Biosensors and Bioelectronics, 2019, 142, 111545.	5.3	4
25	Diffusion impedance modeling for interdigitated array electrodes by conformal mapping and cylindrical finite length approximation. Electrochimica Acta, 2019, 320, 134629.	2.6	4
26	Simultaneous assessment of cell morphology and adhesion using aluminum nanoslit-based plasmonic biosensing chips. Scientific Reports, 2019, 9, 7204.	1.6	12
27	Injection compression molding of transmission-type Fano resonance biochips for multiplex sensing applications. Applied Materials Today, 2019, 16, 72-82.	2.3	10
28	Aluminum Nanostructures for Surface-Plasmon-Resonance-Based Sensing Applications. ACS Applied Nano Materials, 2019, 2, 1930-1939.	2.4	15
29	Combination of an Axicon Fiber Tip and a Camera Device into a Sensitive Refractive Index Sensor. Sensors, 2019, 19, 4911.	2.1	4
30	Polymer LEDs with improved efficacy via periodic nanostructure-based aluminum. Optics Letters, 2019, 44, 4327.	1.7	4
31	96-well capped gold nanoslits for backside-reflection plasmonic biosensing. , 2019, , .		0
32	Fabrication of flexible indium tin oxide-free polymer solar cells with silver nanowire transparent electrode. Japanese Journal of Applied Physics, 2018, 57, 03DD01.	0.8	7
33	Plasmonic Hot-Carriers in Channel-Coupled Nanogap Structure for Metal–Semiconductor Barrier Modulation and Spectral-Selective Plasmonic Monitoring. ACS Photonics, 2018, 5, 2617-2623.	3.2	22
34	Circular Dichroism Control of Tungsten Diselenide (WSe <sub>2</sub> ) Atomic Layers with Plasmonic Metamolecules. ACS Applied Materials & Interfaces, 2018, 10, 15996-16004.	4.0	25
35	Optimization for Gold Nanostructure-Based Surface Plasmon Biosensors Using a Microgenetic Algorithm. ACS Photonics, 2018, 5, 2320-2327.	3.2	25
36	Fabrication and applications of ultraflexible nanostructures using dielectric heating-assisted nanoimprint on PVC films. Current Applied Physics, 2018, 18, 12-18.	1.1	2

#	Article	IF	CITATIONS
37	Dual Sensing Arrays for Surface Plasmon Resonance (SPR) and Surfaceâ€Enhanced Raman Scattering (SERS) Based on Nanowire/Nanorod Hybrid Nanostructures. Advanced Materials Interfaces, 2018, 5, 1801064.	1.9	39
38	<i>Escherichia coli</i> Fiber Sensors Using Concentrated Dielectrophoretic Force with Optical Defocusing Method. ACS Sensors, 2018, 3, 1196-1202.	4.0	9
39	Resonant position tracking method for smartphone-based surface plasmon sensor. Analytica Chimica Acta, 2018, 1032, 99-106.	2.6	20
40	Enhancing Surface Sensing Sensitivity of Metallic Nanostructures using Blue-Shifted Surface Plasmon Mode and Fano Resonance. Scientific Reports, 2018, 8, 9762.	1.6	24
41	Galectin-1 Restricts Vascular Smooth Muscle Cell Motility Via Modulating Adhesion Force and Focal Adhesion Dynamics. Scientific Reports, 2018, 8, 11497.	1.6	28
42	Spectral Imaging Analysis for Ultrasensitive Biomolecular Detection Using Gold-Capped Nanowire Arrays. Sensors, 2018, 18, 2181.	2.1	6
43	Multiplex detection of urinary miRNA biomarkers by transmission surface plasmon resonance. Analyst, The, 2018, 143, 4715-4722.	1.7	26
44	Circular Polarized Emission of Tungsten Diselenide (WSe2) Atomic Layers with Plasmonic Metasurface. , 2018, , .		0
45	Chip-based digital surface plasmon resonance sensing platform for ultrasensitive biomolecular detection. Biosensors and Bioelectronics, 2017, 91, 580-587.	5.3	18
46	Fano resonances in capped metallic nanostructures for highly sensitive plasmonic sensors. , 2017, , .		0
47	Development of radio-frequency heating-assisted nanoimprint with PETG solution for nanostructure-based biosensors. AIP Advances, 2017, 7, .	0.6	2
48	Micro-ellipsometry imaging of biostructures aided by 1D reflection grating. , 2017, , .		0
49	Highly Sensitive Aluminum-Based Biosensors using Tailorable Fano Resonances in Capped Nanostructures. Scientific Reports, 2017, 7, 44104.	1.6	62
50	Enhancing Surface Sensitivity of Nanostructure-Based Aluminum Sensors Using Capped Dielectric Layers. ACS Omega, 2017, 2, 7461-7470.	1.6	14
51	Enhancing angular sensitivity of plasmonic nanostructures using mode transition in hexagonal gold nanohole arrays. Sensors and Actuators B: Chemical, 2017, 241, 800-805.	4.0	6
52	Low-Cost and Rapid Fabrication of Metallic Nanostructures for Sensitive Biosensors Using Hot-Embossing and Dielectric-Heating Nanoimprint Methods. Sensors, 2017, 17, 1548.	2.1	24
53	Electrostatic-field-tunable ferroelectric template for photoreduction of silver nanostructures applied in Raman scattering enhancement. Optical Materials Express, 2017, 7, 2838.	1.6	7
54	Flexible Indium Tin Oxide-Free Polymer Solar Cells with Silver Nanowire Electrodes. Journal of Nanoelectronics and Optoelectronics, 2017, 12, 839-843.	0.1	3

#	Article	IF	CITATIONS
55	Sensitive Detection of Small Particles in Fluids Using Optical Fiber Tip with Dielectrophoresis. Sensors, 2016, 16, 303.	2.1	6
56	Evolution of gold nanoparticle clusters in living cells studied by sectional darkâ€field optical microscopy and chromatic analysis. Journal of Biophotonics, 2016, 9, 738-749.	1.1	8
57	Enhancing the Surface Sensitivity of Metallic Nanostructures Using Oblique-Angle-Induced Fano Resonances. Scientific Reports, 2016, 6, 33126.	1.6	32
58	A compact imaging spectroscopic system for biomolecular detections on plasmonic chips. Analyst, The, 2016, 141, 6126-6132.	1.7	2
59	Quality Detection of Alcoholic Beverages Using Optical Fiber Tips. IEEE Sensors Journal, 2016, 16, 5626-5631.	2.4	4
60	Engineering Chimeric Receptors To Investigate the Size- and Rigidity-Dependent Interaction of PECylated Nanoparticles with Cells. ACS Nano, 2016, 10, 648-662.	7.3	32
61	Visualization of biosensors using enhanced surface plasmon resonances in capped silver nanostructures. Analyst, The, 2016, 141, 974-980.	1.7	4
62	Surface Plasmon Resonance Sensing: Periodic metallic nanostructures for high-sensitivity biosensing applications IEEE Nanotechnology Magazine, 2016, 10, 16-23.	0.9	0
63	Nanoplasmonic biochips for rapid label-free detection of imidacloprid pesticides with a smartphone. Biosensors and Bioelectronics, 2016, 75, 88-95.	5.3	80
64	Ultrahigh density plasmonic hot spots with ultrahigh electromagnetic field for improved photocatalytic activities. Applied Catalysis B: Environmental, 2016, 181, 612-624.	10.8	20
65	Label-Free Detection of Rare Cell in Human Blood Using Gold Nano Slit Surface Plasmon Resonance. Biosensors, 2015, 5, 98-117.	2.3	28
66	Fully integrated Ag nanoparticles/ZnO nanorods/graphene heterostructured photocatalysts for efficient conversion of solar to chemical energy. Journal of Catalysis, 2015, 329, 167-176.	3.1	30
67	A portable grating-based spectrometer for plasmonic biosensing applications. , 2015, , .		0
68	Research on imaging, sensing, and characterization of cells at Research Center for Applied Sciences (RCAS), Academia Sinica. Proceedings of SPIE, 2015, , .	0.8	0
69	Ultra-sensitive and label-free biosensors using surface plasmon resonance of nano-grating structure in nanofluidic preconcentrator. , 2015, , .		0
70	Efficiency enhancement of organic solar cells using peroxo-polytitanic acid coated silver nanowires as transparent electrodes. RSC Advances, 2015, 5, 18990-18996.	1.7	8
71	Chromatogram Analysis on Revealing Aggregated Number and Location of Gold Nanoparticles Within Living Cells. Plasmonics, 2015, 10, 873-880.	1.8	10
72	Ultrasensitive Biosensors Using Enhanced Fano Resonances in Capped Gold Nanoslit Arrays. Scientific Reports, 2015, 5, 8547.	1.6	142

#	Article	IF	CITATIONS
73	Efficiency enhancement of top-illuminated ITO-free organic solar cells using plasmonic-assisted nanostructured reflective electrodes. Journal of Materials Chemistry C, 2015, 3, 9131-9136.	2.7	6
74	Urinary micro-RNA biomarker detection using capped gold nanoslit SPR in a microfluidic chip. Analyst, The, 2015, 140, 4097-4104.	1.7	34
75	Creating Optical Near-Field Orbital Angular Momentum in a Gold Metasurface. Nano Letters, 2015, 15, 2746-2750.	4.5	113
76	Determination of the effective index and thickness of biomolecular layer by Fano resonances in gold nanogrid array. Optics Express, 2015, 23, 21596.	1.7	11
77	Ultraviolet-enhanced room-temperature gas sensing by using floccule-like zinc oxide nanostructures. Applied Physics Letters, 2015, 106, .	1.5	14
78	Creating Surface Plasmon Orbital Angular Momentum in a Gold Metasurface. , 2015, , .		0
79	Dose dependent distribution and aggregation of gold nanoparticles within human lung adeno-carcinoma cells. RSC Advances, 2015, 5, 98309-98317.	1.7	2
80	Plasmonic Nanoslit Arrays for Sensitive Biosensors. Topics in Applied Physics, 2015, , 447-468.	0.4	2
81	Enhanced detection sensitivity of higher-order vibrational modes of gold nanodisks on top of a GaN nanorod array through localized surface plasmons. Applied Physics Letters, 2014, 105, .	1.5	6
82	Photoactivated Metal-Oxide Gas Sensing Nanomesh by Using Nanosphere Lithography. Materials Research Society Symposia Proceedings, 2014, 1675, 139-144.	0.1	0
83	Dual SPR-SERS Sensors Using Gold Nanoslits and Oblique Angle Deposition. , 2014, , .		0
84	Pâ€61: WITHDRAWN: Pâ€62: Brightness and Contrast Improvement of Display Panel by Using Antireflection Films Nanoimprinted by Densityâ€Graded Nanoporous Silicon. Digest of Technical Papers SID International Symposium, 2014, 45, 1212-1215.	0.1	0
85	Pâ€63: Highly Transparent and Rub Resistive Nanostructured Diamondâ€like Carbon Protective Coatings for Display Application. Digest of Technical Papers SID International Symposium, 2014, 45, 1216-1219.	0.1	1
86	Preface to Special Topic: Selected Papers from the Advances in Microfluidics and Nanofluidics 2014 Conference in Honor of Professor Hsueh-Chia Chang's 60th Birthday. Biomicrofluidics, 2014, 8, 051901.	1.2	0
87	Fabrication of Transparent Electrodes with Silver Nanowires and PPT Gel for Organic Optoelectronic Devices. Materials Research Society Symposia Proceedings, 2014, 1699, 25.	0.1	0
88	The effect of acidic pH on the inhibitory efficacy of peptides against the interaction ICAM-1/LFA-1 studied by surface plasmon resonance (SPR). Biosensors and Bioelectronics, 2014, 56, 159-166.	5.3	6
89	Enhancing surface plasmon polariton propagation by two-layer dielectric-loaded waveguides on silver surface. Applied Physics A: Materials Science and Processing, 2014, 115, 93-98.	1.1	5
90	Efficiency improvement of organic bifunctional devices by applying omnidirectional antireflection nanopillars. RSC Advances, 2014, 4, 9588.	1.7	5

#	Article	IF	CITATIONS
91	Spectral and mode properties of surface plasmon polariton waveguides studied by near-field excitation and leakage-mode radiation measurement. Nanoscale Research Letters, 2014, 9, 430.	3.1	5
92	Enhancing detection sensitivity of metallic nanostructures by resonant coupling mode and spectral integration analysis. Optics Express, 2014, 22, 19621.	1.7	9
93	Efficiency enhancement of organic light-emitting devices by using honeycomb metallic electrodes and two-dimensional photonic crystal arrays. Organic Electronics, 2014, 15, 3043-3051.	1.4	13
94	Ultrahighâ€Density Plasmonicâ€Nanoparticle‣ensitized Semiconductor Photocatalysts Profit from Cooperative Light Harvesting and Charge Separation Processes: Experiments, Simulations, and Multifunctional Plasmonics. Particle and Particle Systems Characterization, 2014, 31, 895-907.	1.2	3
95	Tunable Fano resonance in two-layer gold nanoslit array and its application for highly sensitive biosensors. , 2014, , .		1
96	Dynamic Monitoring of Mechano-Sensing of Cells by Gold Nanoslit Surface Plasmon Resonance Sensor. PLoS ONE, 2014, 9, e89522.	1.1	9
97	Transparent electrode for organic solar cells using multilayer structures with nanoporous silver film. Solar Energy Materials and Solar Cells, 2013, 118, 81-89.	3.0	25
98	Optofluidic Platform for Realâ€Time Monitoring of Live Cell Secretory Activities Using Fano Resonance in Gold Nanoslits. Small, 2013, 9, 3532-3540.	5.2	52
99	Ultrasensitive biosensors using Fano resonances in double-layer gold nanostructures. , 2013, , .		1
100	High-Throughput Label-Free Detection Using a Gold Nanoslit Array With 2-D Spectral Images and Spectral Integration Methods. IEEE Journal of Selected Topics in Quantum Electronics, 2013, 19, 4800407-4800407.	1.9	2
101	Magnetic nanoparticle-enhanced SPR on gold nanoslits for ultra-sensitive, label-free detection of nucleic acid biomarkers. Analyst, The, 2013, 138, 2740.	1.7	37
102	P.116: Light Extraction Improvement of Flexible Topâ€Emitting Organic Lightâ€Emitting Devices by Using Nanoimprinted Periodically Corrugated Polycarbonate Substrate. Digest of Technical Papers SID International Symposium, 2013, 44, 1421-1423.	0.1	0
103	Increased detection sensitivity of surface plasmon sensors using oblique induced resonant coupling. Optics Letters, 2013, 38, 4962.	1.7	12
104	Enhanced light out-coupling of organic light-emitting diode using metallic nanomesh electrodes and microlens array. Optics Express, 2013, 21, 8535.	1.7	39
105	Omnidirectional antireflection polymer films nanoimprinted by density-graded nanoporous silicon and image improvement in display panel. Optics Express, 2013, 21, 29827.	1.7	9
106	Cell viability monitoring using Fano resonance in gold nanoslit array. Applied Physics Letters, 2013, 103, .	1.5	17
107	P.115: Micropyramid Array with Antireflective Nanostructure Surfaces for Light Extraction Efficiency Enhancement of Organic Light Emitting Devices. Digest of Technical Papers SID International Symposium, 2013, 44, 1417-1420.	0.1	1
108	Comparison of light out-coupling enhancements in single-layer blue-phosphorescent organic light emitting diodes using small-molecule or polymer hosts. Journal of Applied Physics, 2013, 114, 173106.	1.1	8

#	Article	IF	CITATIONS
109	Strong suppression of angle and period dependency of surface-plasmon-polaritons in gold nanodisks by combining a nanorod substrate. , 2013, , .		0
110	Enhanced localized plasmonic detections using partially-embedded gold nanoparticles and ellipsometric measurements. Biomedical Optics Express, 2012, 3, 899.	1.5	42
111	Improve efficiency of white organic light-emitting diodes by using nanosphere arrays in color conversion layers. Optics Express, 2012, 20, 3005.	1.7	10
112	Refractive index profiling of an optical waveguide from the determination of the effective index with measured differential fields. Optics Express, 2012, 20, 26766.	1.7	17
113	Near-field dynamic study of the nanoacoustic effect on the extraordinary transmission in gold nanogratings. Optics Express, 2012, 20, 16186.	1.7	8
114	Pâ€117: High Efficient Color Conversion Layers for White Organic Lightâ€Emitting Diodes using Polystyrene Nanosphere Monolayers. Digest of Technical Papers SID International Symposium, 2012, 43, 1499-1502.	0.1	1
115	Pâ€122: Luminous and Conversion Efficiency Improvement in OLED/OPV Tandem Device with Omnidirectional Antireflection Nanopillars. Digest of Technical Papers SID International Symposium, 2012, 43, 1516-1519.	0.1	1
116	Optimization of polymer light emitting devices using TiOx electron transport layers and prism sheets. Organic Electronics, 2012, 13, 2667-2670.	1.4	4
117	Comparison of transmission and reflection spectrum of angular dependent surface plasmon resonances of gold nanoslits. , 2012, , .		0
118	Enhancing Surface Plasmon Detection Using Template-Stripped Gold Nanoslit Arrays on Plastic Films. ACS Nano, 2012, 6, 2931-2939.	7.3	146
119	Improving Surface Plasmon Detection in Gold Nanostructures Using a Multiâ€Polarization Spectral Integration Method. Advanced Materials, 2012, 24, OP253-9.	11.1	23
120	Intense Near-Field Interaction between Surface Plasmon Polaritons and Nanoacoustic Pulses. , 2012, , .		0
121	Optimization of periodic gold nanostructures for intensity-sensitive detection. Applied Physics Letters, 2011, 99, 083108.	1.5	16
122	Ellipsometry study on gold-nanoparticle-coated gold thin film for biosensing application. Biomedical Optics Express, 2011, 2, 2569.	1.5	27
123	Efficiency enhancement of flexible organic light-emitting devices by using antireflection nanopillars. Optics Express, 2011, 19, A295.	1.7	22
124	Sensitive biosensors using Fano resonance in single gold nanoslit with periodic grooves. Optics Express, 2011, 19, 24530.	1.7	59
125	Investigation of surface plasmon biosensing using gold nanoparticles enhanced ellipsometry. Optics Letters, 2011, 36, 775.	1.7	21
126	Refractive index measurement of optical waveguides using modified end-fire coupling method. Optics Letters, 2011, 36, 2008.	1.7	11

#	Article	IF	CITATIONS
127	Pâ€179: Efficiency Enhancement of PLED by Using TiO <sub>x</sub> Electron Transport Layer with Prism Sheet Attachment. Digest of Technical Papers SID International Symposium, 2011, 42, 1770-1772.	0.1	0
128	Pâ€113: Efficiency and Image Enhancement of Flexible Organic Lightâ€Emitting Devices by Using Antireflection Nanopillars. Digest of Technical Papers SID International Symposium, 2011, 42, 1531-1534.	0.1	0
129	Plasmonic biosensing with nanoimprint binary grating using ellipsometry. , 2011, , .		2
130	Structure Effect on Sensitivity of Gold Nanoslits Studied by Spectral Integration Method. Plasmonics, 2011, 6, 483-490.	1.8	4
131	Near-Field Coupling Method for Subwavelength Surface Plasmon Polariton Waveguides. Plasmonics, 2011, 6, 557-563.	1.8	5
132	Fabrication of gold sub-wavelength pore array using gas-assisted hot embossing with anodic aluminum oxide (AAO) template. Microelectronic Engineering, 2011, 88, 909-913.	1.1	8
133	Transparent and conductive metallic electrodes fabricated by using nanosphere lithography. Organic Electronics, 2011, 12, 961-965.	1.4	49
134	Large-area Raman enhancement substrates using spontaneous dewetting of gold films and silver nanoparticles deposition. Sensors and Actuators B: Chemical, 2011, 156, 245-250.	4.0	9
135	Novel fabrication of an Au nanocone array on polycarbonate for high performance surface-enhanced Raman scattering. Journal of Micromechanics and Microengineering, 2011, 21, 035023.	1.5	10
136	Local plasmonic resonance based biosensor for investigating DNA hybridization using ellipsometry. , 2010, , .		3
137	Color Variation in Periodic Ag Line Arrays Patterned by Using Electron-Beam Lithography. Journal of Nanoscience and Nanotechnology, 2010, 10, 4581-4585.	0.9	2
138	Pâ€156: Transparent Conductive Electrodes Based on Patterned Silver Thin Film by Nanosphere Lithography. Digest of Technical Papers SID International Symposium, 2010, 41, 1834-1836.	0.1	0
139	Development of a Controlled Environment Nearâ€Field Optical Microscope for Organic Thin Film Studies. Journal of the Chinese Chemical Society, 2010, 57, 469-477.	0.8	1
140	Cesium doped and undoped ZnO nanocrystalline thin films: a comparative study of structural and microâ€Raman investigation of optical phonons. Journal of Raman Spectroscopy, 2010, 41, 1594-1600.	1.2	44
141	Surface plasmon resonance ellipsometry based sensor for studying biomolecular interaction. Biosensors and Bioelectronics, 2010, 25, 2633-2638.	5.3	26
142	Size-dependent endocytosis of gold nanoparticles studied by three-dimensional mapping of plasmonic scattering images. Journal of Nanobiotechnology, 2010, 8, 33.	4.2	235
143	Enhancing Surface Plasmon Detection Using Ultrasmall Nanoslits and a Multispectral Integration Method. Small, 2010, 6, 1900-1907.	5.2	53
144	Verifying expressed transcript variants by detecting and assembling stretches of consecutive exons. Nucleic Acids Research, 2010, 38, e187-e187.	6.5	2

#	Article	IF	CITATIONS
145	High sensitive protein fluorescence sensing on nano ring gap (NRG) LSPR sensor. , 2010, , .		0
146	Femtosecond laser-ultrasonic investigation of plasmonic fields on the metal/gallium nitride interface. Applied Physics Letters, 2010, 97, .	1.5	12
147	Multispectral Refractive Index Sensing Using Surface Plasmon Resonance on Gold Nanoslits. Materials Research Society Symposia Proceedings, 2010, 1253, 26.	0.1	0
148	Sensitive liquid refractive index sensors using tapered optical fiber tips. Optics Letters, 2010, 35, 944.	1.7	69
149	Optical metrology of randomly-distributed Au colloids on a multilayer film. Optics Express, 2010, 18, 1310.	1.7	7
150	Giant birefringence induced by plasmonic nanoslit arrays. Applied Physics Letters, 2009, 95, .	1.5	41
151	Giant birefringence induced by plasmonic nanowire arrays. , 2009, , .		0
152	Study of gold nanoparticles and live cells interactions by using planar evanescent wave excitation. Journal of Biomedical Optics, 2009, 14, 021005.	1.4	4
153	Morphological studies of living cells using gold nanoparticles and dark-field optical section microscopy. Journal of Biomedical Optics, 2009, 14, 1.	1.4	18
154	One-Dimensional Dynamics and Transport of DNA Molecules in a Quasi-Two-Dimensional Nanoslit. Macromolecules, 2009, 42, 1770-1774.	2.2	32
155	Focusing subwavelength light by using nanoholes in a transparent thin film. Optics Letters, 2009, 34, 1867.	1.7	11
156	Intensity sensitivity of gold nanostructures and its application for high-throughput biosensing. Optics Express, 2009, 17, 23104.	1.7	46
157	Comparisons of Surface Plasmon Sensitivities in Periodic Gold Nanostructures. Plasmonics, 2008, 3, 119-125.	1.8	43
158	Optical nanometrology of Au nanoparticles on a multilayer film. Physica Status Solidi C: Current Topics in Solid State Physics, 2008, 5, 1194-1197.	0.8	3
159	Sensitive label-free biosensors by using gap plasmons in gold nanoslits. Biosensors and Bioelectronics, 2008, 24, 210-215.	5.3	31
160	Observation of nanoparticle internalization on cellular membranes by using noninterferometric widefield optical profilometry. Applied Optics, 2008, 47, 2458.	2.1	7
161	Extraction enhancement in organic light emitting devices by using metallic nanowire arrays. Applied Physics Letters, 2008, 92, .	1.5	47
162	Single live cell refractometer using nanoparticle coated fiber tip. Applied Physics Letters, 2008, 93, .	1.5	25

#	Article	IF	CITATIONS
163	Magnetization reversal in epitaxial MnAs thin films. Journal of Applied Physics, 2008, 104, 033921.	1.1	3
164	Pâ€113: Temporal Behavior of Nanostructure Formation in Photopolymer on Back Light Layer of TFT‣ED. Digest of Technical Papers SID International Symposium, 2008, 39, 1614-1617.	0.1	0
165	29.4: Extraction Enhancement and Lateral Cavity Effect of Organic Light Emitting Diode by Using Metallic Nanostructures. Digest of Technical Papers SID International Symposium, 2008, 39, 415-418.	0.1	0
166	Three-dimensional motion of a nanoparticle on the cell membrane observed by non-interferometric widefield optical profilometry. , 2008, , .		0
167	Comparisons of the surface plasmon sensitivities for nanohole and nanoslit arrays. Proceedings of SPIE, 2007, , .	0.8	3
168	Static conformation and dynamics of single DNA molecules confined in nanoslits. Physical Review E, 2007, 76, 011806.	0.8	64
169	Sensitive detection of nanoparticles using metallic nanoslit arrays. Applied Physics Letters, 2007, 90, 233119.	1.5	13
170	Sub-100 nm photolithography using TE-polarized waves in transparent nanostructures. Optics Letters, 2007, 32, 71.	1.7	7
171	Fabrication of a close-packed hemispherical submicron lens array and its application in photolithography. Optics Express, 2007, 15, 6774.	1.7	10
172	Investigation on the Correlation Between the Crystalline and Optical Properties of InGaN Using Near-Field Scanning Optical Microscopy. Electrochemical and Solid-State Letters, 2007, 10, H217.	2.2	1
173	Sensitive biosensor array using surface plasmon resonance on metallic nanoslits. Journal of Biomedical Optics, 2007, 12, 044023.	1.4	118
174	Two-dimensional refractive index profiling by using differential near-field scanning optical microscopy. Applied Physics Letters, 2007, 91, 061123.	1.5	16
175	Coupled waveguide–surface plasmon resonance biosensor with subwavelength grating. Biosensors and Bioelectronics, 2007, 22, 2737-2742.	5.3	51
176	Characterization and application of single fluorescent nanodiamonds as cellular biomarkers. Proceedings of the National Academy of Sciences of the United States of America, 2007, 104, 727-732.	3.3	810
177	Fabricating subwavelength array structures using a near-field photolithographic method. Applied Physics Letters, 2006, 88, 101109.	1.5	7
178	Optical waveguide biosensors constructed with subwavelength gratings. Applied Optics, 2006, 45, 1938.	2.1	30
179	Plasmon-enhanced optical waveguide biosensors constructed with sub-wavelength gold grating. , 2006, , .		2
180	Coupled waveguide-surface plasmon resonance biosensors constructed with sub-wavelength grating.		1

, 2006, , . 180

#	Article	IF	CITATIONS
181	Conjugation of Î <sup>3</sup> -Fe2O3 nanoparticles with single strand oligonucleotides. Journal of Magnetism and Magnetic Materials, 2006, 304, e412-e414.	1.0	14
182	Fabrication of photonic bandgap structures with designed defects by edge diffraction lithography. Nanotechnology, 2006, 17, 1333-1338.	1.3	1
183	Nanofiber optic sensor based on the excitation of surface plasmon wave near fiber tip. Journal of Biomedical Optics, 2006, 11, 014032.	1.4	32
184	Sensitive plasmonic biosensor using gold nanoparticles on a nano fiber tip. , 2006, 6099, 86.		0
185	Magnetic induced optical transmittance study of monodisperse nano-size FePt ferrofluid. , 2006, , .		Ο
186	A label-free optical waveguide biosensor with sub-wavelength gratings. , 2005, 6007, 234.		1
187	Light emission in phase separated conjugated and non-conjugated polymer blends. Polymer, 2005, 46, 4967-4970.	1.8	24
188	Beaming effect of optical near-field in multiple metallic slits with nanometric linewidth and micrometer pitch. Optics Communications, 2005, 253, 198-204.	1.0	7
189	Near-field photolithographic method for making two dimensional photonic bandgap structures. , 2005, , .		0
190	Near-field magneto-optical microscopy using surface-plasmon waves and the transverse magneto-optical Kerr effect. Journal of Applied Physics, 2005, 98, 093904.	1.1	2
191	Off-angle illumination induced surface plasmon coupling in subwavelength metallic slits. Optics Express, 2005, 13, 10784.	1.7	16
192	Polarization dependence of light intensity distribution near a nanometric aluminum slit. Journal of the Optical Society of America B: Optical Physics, 2004, 21, 1005.	0.9	12
193	A Novel Wet-Etching Method Using Electric-Field-Assisted Proton Exchange in LiNbO <tex>\$_3\$</tex> . Journal of Lightwave Technology, 2004, 22, 1764-1771.	2.7	24
194	Subwavelength focusing in the near field in mesoscale air–dielectric structures. Optics Letters, 2004, 29, 433.	1.7	16
195	Systematic variation of polymer jacketed fibres and the effects on tip etching dynamics. Journal of Microscopy, 2003, 210, 334-339.	0.8	18
196	Diffraction-induced near-field optical images in mesoscale air–dielectric structures. Journal of the Optical Society of America B: Optical Physics, 2003, 20, 1503.	0.9	15
197	Room temperature vibrational photoluminescence and field emission of nanoscaled tris-(8-hydroxyquinoline) aluminum crystalline film. Applied Physics Letters, 2003, 83, 4607-4609.	1.5	42
198	Determination of mesoscale crystallization by collection-mode polarization modulated near-field optical microscopy. Review of Scientific Instruments, 2002, 73, 2624-2628.	0.6	6

#	Article	IF	CITATIONS
199	Optical near field in nanometallic slits. Optics Express, 2002, 10, 1418.	1.7	28
200	The morphological dependence of charge transport in a soluble luminescent conjugated polymer. Organic Electronics, 2002, 3, 81-88.	1.4	40
201	Soluble Electroluminescent Poly(phenylene vinylene)s with Balanced Electron- and Hole Injections. Journal of the American Chemical Society, 2001, 123, 2296-2307.	6.6	274
202	The correlation between polarization modulated near-field optical images and the anisotropy of the probe. Journal of Microscopy, 2001, 202, 148-153.	0.8	8
203	Mesoscale structures in luminescent conjugated polymer thin films studied by near-field scanning optical microscopy. Journal of Physics and Chemistry of Solids, 2001, 62, 1643-1655.	1.9	18
204	Polarization anisotropy in mesoscale domains of poly(phenylene vinylene) thin films. Physical Review B, 2001, 63, .	1.1	18
205	The effect of humidity on probe-sample interactions in near-field scanning optical microscopy. Journal of Applied Physics, 2000, 87, 2561-2564.	1.1	19
206	Study of conjugated polymer blend films by a near field scanning optical microscopy. Synthetic Metals, 1999, 102, 1209-1210.	2.1	12
207	A novel self-aligned fabrication process for nickel-indiffused lithium niobate ridge optical waveguides. Journal of Lightwave Technology, 1999, 17, 613-620.	2.7	2
208	Determination of the shear force magnitude in near-field scanning optical microscopy. Ultramicroscopy, 1998, 71, 159-163.	0.8	4
209	The inhomogeneity in conjugated polymer blend films. Ultramicroscopy, 1998, 71, 263-267.	0.8	10
210	Large scanning area near field optical microscopy. Review of Scientific Instruments, 1998, 69, 3614-3617.	0.6	3
211	The probe dynamics under shear force in near-field scanning optical microscopy. Journal of Applied Physics, 1998, 83, 3461-3468.	1.1	21
212	Nanometer scale mixing homogeneity in light emitting polymer blend thin films. Journal of Applied Physics, 1998, 83, 1782-1784.	1.1	11
213	Tip-sample distance regulation for near-field scanning optical microscopy using the bending angle of the tapered fiber probe. Journal of Applied Physics, 1998, 84, 4655-4660.	1.1	8
214	Vibration dynamics of tapered optical fiber probes. Journal of Applied Physics, 1997, 81, 1623-1627.	1.1	31
215	Phase separation in polyaniline with near-field scanning optical microscopy. Applied Optics, 1997, 36, 3301.	2.1	6
216	Surface modification of conjugated polymers: an application of near-field optical microscopy in sub-micron photochemistry. Synthetic Metals, 1997, 85, 1421-1422.	2.1	5

#	Article	IF	CITATIONS
217	Two-dimensional near-field intensity distribution of tapered fiber probes. Optics Letters, 1996, 21, 1876.	1.7	7
218	Surface modification and patterning of conjugated polymers with near-field optical microscopy. Advanced Materials, 1996, 8, 573-576.	11.1	41
219	<title>Method to increase brightness of the tapered fiber probe for scanning near-field optical microscope</title> . , 1995, , .		0
220	<title>Conjugated polymer studies by near-field scanning optical microscope</title> . , 1995, , .		0
221	Simultaneous reflection and transmission modes near-field scanning optical microscope. Ultramicroscopy, 1995, 61, 237-239.	0.8	2
222	Direct measurements of the true vibrational amplitudes in shear force microscopy. Applied Physics Letters, 1995, 67, 3835-3837.	1.5	40
223	Conductivity Relaxation of 1-Methyl-2-pyrrolidone-Plasticized Polyaniline Film. Macromolecules, 1995, 28, 7645-7652.	2.2	72
224	A novel couple-type power divider with large-angle low-loss characteristics. IEEE Journal of Quantum Electronics, 1995, 31, 735-742.	1.0	6
225	Novel TE-TM mode splitter on lithium niobate using nickel indiffusion and proton exchange techniques. Electronics Letters, 1994, 30, 35-37.	0.5	8
226	Fabrication of lithium niobate optical channel waveguides by nickel indiffusion. Microwave and Optical Technology Letters, 1994, 7, 219-221.	0.9	10
227	A TE-TM mode splitter on lithium niobate using Ti, Ni, and MgO diffusions. IEEE Photonics Technology Letters, 1994, 6, 245-248.	1.3	66
228	Design and application of very low-loss abrupt bends in optical waveguides. IEEE Journal of Quantum Electronics, 1994, 30, 2827-2835.	1.0	24
229	Beam propagation analysis of a tapered proton-exchanged lithium niobate optical waveguide. , 1994, 4, 40-42.		3
230	A new iterative method for the analysis of longitudinally invariant waveguide couplers. Journal of Lightwave Technology, 1994, 12, 2056-2065.	2.7	7
231	Fabrication of magnesium-oxide-induced lithium outdiffusion waveguides. IEEE Photonics Technology Letters, 1992, 4, 872-875.	1.3	9
232	A new approach to the analysis of the soliton: Nonuniform finite difference beam propagation method. Microwave and Optical Technology Letters, 1992, 5, 284-288.	0.9	1
233	Fabrication of strip loaded outdiffusion guides on lithium niobate substrate. Microwave and Optical Technology Letters, 1992, 5, 309-313.	0.9	1
234	A Mach-Zehnder interferometer made of strip-loaded outdiffusion guide. Microwave and Optical Technology Letters, 1992, 5, 611-613.	0.9	0

#	Article	IF	CITATIONS
235	Evanescent planar wave system for reading DNA microarrays on thin glass slides. , 0, , .		0
236	Edge diffraction induced near-field contrast in subwavelength structures. , 0, , .		0
237	Direct Detection of Virus-Like Particles Using Color Images of Plasmonic Nanostructures. Optics Express, 0, , .	1.7	1